Dehydration in the tropical tropopause layer: Implications from the UARS Microwave Limb Sounder

Dehydration in the tropical tropopause layer: Implications from the UARS Microwave Limb Sounder

W. G. Read, D. L. Wu, and J. W. Waters
Jet Propulsion Laboratory, California Institute of Technology, Pasadena, California, USA

H. C. Pumphrey
Department of Meteorology, University of Edinburgh, Edinburgh, UK

Received 8 August 2003; revised 9 January 2004; accepted 3 February 2004; published 26 March 2004.

[1] Measurements of H_2O from the Microwave Limb Sounder (MLS) on the Upper Atmosphere Research Satellite (UARS) are used to investigate the structure of H_2O in the near tropopause region and dehydration mechanisms in the tropical tropopause layer (TTL). The new MLS data are consistent with convective input of H_2O into the bottom of the TTL followed by slow ascent with a maximum relative amplitude in the seasonal cycle occurring near the tropopause nearly in phase with the tropopause temperature seasonal cycle. The relative amplitude of the seasonal cycle shows a minimum at 121 hPa in the upwelling moist phase. These features are reproduced with the "cold-trap" dehydration hypothesis. Seasonal maps show wettest tropical 100 hPa H_2O colocated with continental convection. *INDEX TERMS:* 3362 Meteorology and Atmospheric Dynamics: Stratosphere/troposphere interactions; 3314 Meteorology and Atmospheric Dynamics: Convective processes; 3374 Meteorology and Atmospheric Dynamics: Tropical meteorology; *KEYWORDS:* UARS Microwave Limb Sounder water vapor measurements, dehydration in the tropical tropopause layer, seasonal evolution of water vapor in the upper troposphere/lower stratosphere

Citation: Read, W. G., D. L. Wu, J. W. Waters, and H. C. Pumphrey (2004), Dehydration in the tropical tropopause layer: Implications from the UARS Microwave Limb Sounder, *J. Geophys. Res.*, *109*, D06110, doi:10.1029/2003JD004056.

1. Introduction

[2] There is general agreement that water vapor enters the stratosphere in the tropics [e.g., *Holton et al.*, 1995]. Moist boundary layer air is rapidly transported upward by deep convection into the tropical tropopause layer (TTL), a region between the troposphere and stratosphere extending from the zero net radiative heating level (~355 K potential temperature, 150 hPa pressure, 13 km height) to the highest level that convection reaches (~420–450 K, 70 hPa, 18–20 km) [*Sherwood and Dessler*, 2000]. Tropical average water vapor concentrations at 13 km are ~18.5 ppmv, near saturation with respect to ice [*Jensen et al.*, 1999; *Read et al.*, 2001], but air rising out of the TTL into the stratosphere contains only ~4 ppmv H_2O [e.g., *Dessler and Kim*, 1999]. The processes by which air is dehydrated in the TTL are inadequately understood at present, and two hypotheses have emerged that appear to be most consistent with the available data. "Convective dehydration" [*Sherwood and Dessler*, 2001] posits that air emerges from convection fully dehydrated (on average) to stratospheric values. "Cold-trap dehydration" [*Holton and Gettelman*, 2001] posits that slowly ascending air is dehydrated in situ to stratospheric values by repeated exposure to the lowest TTL temperatures through rapid horizontal transport. Better understanding of dehydration processes in the TTL is needed, for example to help understand the causes for increasing stratospheric H_2O [e.g., *Rosenlof et al.*, 2001] and assess implications for future climate change and recovery of the ozone layer. Causes of the stratospheric H_2O increase to date cannot be explained either by observed increases in CH_4 [*Kley et al.*, 2000] or decreases in tropopause temperatures [*Randel et al.*, 2000; *Seidel et al.*, 2001]. The increase may be related to biomass burning [*Sherwood*, 2002] or to changes in upward transport of H_2O [*Rosenlof*, 2002]. It has been recently reported that the increase in stratospheric H_2O has slowed [*Nedoluha et al.*, 2003].

2. Observational Data

[3] The new MLS V7.02 H_2O product is used in the analysis here. The production, estimated accuracy and quality of this data product is described by *Read et al.* [2004]. The MLS V7.02 retrieved from the 183 GHz radiometer provides H_2O profiles in the tropical upper troposphere and lower stratosphere. Data for most days from 19 September 1991 to 24 April 1993, the lifetime of the 183 GHz radiometer, are available. The MLS measures ~1300 profiles per day between 81°S and 34°N or 34°S and 81°N depending on the Upper Atmosphere Research Satellite (UARS) yaw configuration. Descriptions of the UARS and MLS are given elsewhere [*Reber*, 1993; *Barath et al.*, 1993; *Waters et al.*, 1999]. MLS V7.02 data have H_2O on 316, 261, 215, 177, 146, 121, 100, 83, 68, 56, and 46 hPa. The vertical resolution of this data set is 3–4 km. In this

0148-0227/04/2003JD004056

analysis we use the MLS V7.02 data on the levels between 147 to 56 hPa. MLS V4.9 upper tropospheric humidity (UTH) [*Read et al.*, 2001] and MLS V0104 stratospheric H_2O [*Pumphrey*, 1999], two previously released MLS versions, are used for pressures greater than 147 and less than 56 hPa, respectively. The full vertical range of H_2O profiles shown in this study use retrievals from the 183 GHz radiometer for pressure levels equal to or less than 147 hPa and retrievals from the 203 GHz radiometer are for pressures greater than 147 hPa. Comparisons with the Halogen Occultation Experiment (HALOE) [*Russell et al.*, 1993] V19 and the National Oceanic and Atmospheric Administration (NOAA), Climate Monitoring and Diagnostics Laboratory (CMDL) frost-point hygrometer (data provided by NOAA/CMDL) indicate that the MLS V7.02 data show good agreement in the seasonal evolution of the zonal means and accurate within 10% at 121, 83, 68, and 56 hPa but have dry biases of 30% and 20% at 147 and 100 hPa, respectively. In the analysis to follow we have increased the MLS V7.02 147 and 100 hPa data by 30% and 20%, respectively. MLS can make measurements under most cloudy situations encountered in the upper troposphere with only ~1% of the tropical data being rejected.

3. Results

[4] Here we discuss results from an analysis of the V7.02 H_2O data, with emphasis on dehydration in the TTL. The "convective" and "cold-trap" hypotheses for TTL dehydration have different implications for the distribution of H_2O in this region. The "convective" hypothesis implies smallest values of H_2O downwind of deep convection and a vertical distribution that has a maximum relative amplitude of the seasonal cycle beginning near the base of the TTL [*Sherwood and Dessler*, 2003]. The "cold-trap" hypothesis implies smallest values of H_2O in the vicinity and downwind of lowest temperatures in the TTL and a vertical distribution having a maximum relative amplitude of the seasonal cycle near the cold point tropopause [*Holton and Gettelman*, 2001].

[5] The transition from the troposphere to the stratosphere as seen in MLS H_2O is shown in Figure 1 for the temporal evolution of the zonal mean at several altitudes. The upper tropospheric levels, between 316–147 hPa, behave similarly (there is a data discontinuity on the 147 hPa surface in May 1993, when the H_2O data switches from V7.02 to the noisier V4.9). As noted for 215 hPa H_2O by *Elson et al.* [1996], the latitude of the upper tropospheric moisture maximum follows the solar annual cycle with a 2 month lag, with the tropical maximum higher in April–September than other months. The April temporal maximum in H_2O at the equator may be associated with a maximum in tropical upper tropospheric temperatures [*Yulaeva et al.*, 1994; *Reed and Vleck*, 1969] that occurs in March. The seasonal amplitude in temperature is <0.5 K and the observed increase in H_2O (20–30%) is much larger than that implied by a temperature change at constant relative humidity (6%). The moisture maximum in the zonal means at 316–147 hPa is caused by rapid vertical transport of boundary layer H_2O (with freeze drying) in deep convection that occurs in the tropics and also follows the solar cycle with a 2 month lag. The solar tracking of the zonal H_2O maximum weakens at 121 hPa and eventually disappears at 83 hPa. An H_2O maximum during the Indian monsoon period is seen in August 1992 at 20°N penetrating as high as 83 hPa. Some caution should be exercised in interpreting this as evidence that the Indian monsoon penetrates to 83 hPa because the vertical smearing of the data is 4 km. Another feature seen at 121–83 hPa is the northward displacement with increasing height of the maximum amplitude in the annual cycle. This is also seen in the HALOE data [*Randel et al.*, 2001]. Figure 1 shows that the lowest zonal mean H_2O values occur in the vicinity of 100–83 hPa, 20–25°N in January–February. Above 83 hPa, the H_2O zonal mean annual cycle amplitude is symmetric about the equator between 40°S and 40°N.

[6] Figure 2 shows the evolution of the 12°S to 12°N area average vertical distribution of the H_2O anomaly between early October 1991 and middle April 1993, as seen by MLS with inclusion of the V7.02 data. The results are presented as percentage differences from the average value for this period at each pressure level. The V4.9 data, used at 215 hPa and higher pressures, were quality screened according to *Read et al.* [2001], with values exceeding 120% relative humidity with respect to ice (%RHi) set to 100%RHi. V0104 data are used at 46 hPa and lower pressures. The plotted values are daily averages that have been smoothed over 30 days at 464 and 316 hPa, 20 days at 215 hPa, and 10 days at 147 hPa and lower pressures. The smoothing helps remove considerable tropospheric meteorological variability and fills some daily data gaps.

[7] A dominant feature in Figure 2 is the tropical "tape recorder" identified by *Mote et al.* [1995] at pressures of 100 hPa and lower. The "tape recorder" is the imprint of the tropopause temperature on H_2O undergoing slow vertical ascent [*Mote et al.*, 1996]. The V7.02 H_2O data show a feature resembling slow vertical ascent extending down to 147 hPa, and connecting with a seasonal cycle in tropical H_2O at 147–464 hPa (the lower altitude limit of MLS H_2O measurements). Figure 1 shows that the seasonal cycle in tropical H_2O at 147–464 hPa seen in Figure 2 repeats annually. It follows the seasonal cycle in upper tropospheric temperatures with a one month lag. This H_2O seasonal cycle is not likely to be a retrieval artifact caused by the temperature cycle because the temperature variation amplitude of 0.5 K would cause a retrieved H_2O artifact of not more than 2.5%, small compared to the observed amplitude of ~25%.

[8] We now compare the MLS time-height zonal mean H_2O observations with results from the *Holton and Gettelman* [2001] two-dimensional (2-D) TTL model. The two-dimensional (longitude-height) model requires as inputs an annually varying temperature distribution, zonal mean horizontal and vertical wind components and the humidity at the base altitude in the model. The model predicts the 2-D evolution of H_2O and ice amounts. The longitude coordinate is an 18000 km circulating loop. The altitude range is from 14–19 km with a tropopause fixed at 16.5 km. The background horizontal and upward vertical wind velocities are 10 m s^{-1} and 0.3 mm s^{-1}. Temperature is specified by the daily United Kingdom Meteorological Office (UKMO) analysis. The UKMO analysis captures the phase shift of the maximum tem-

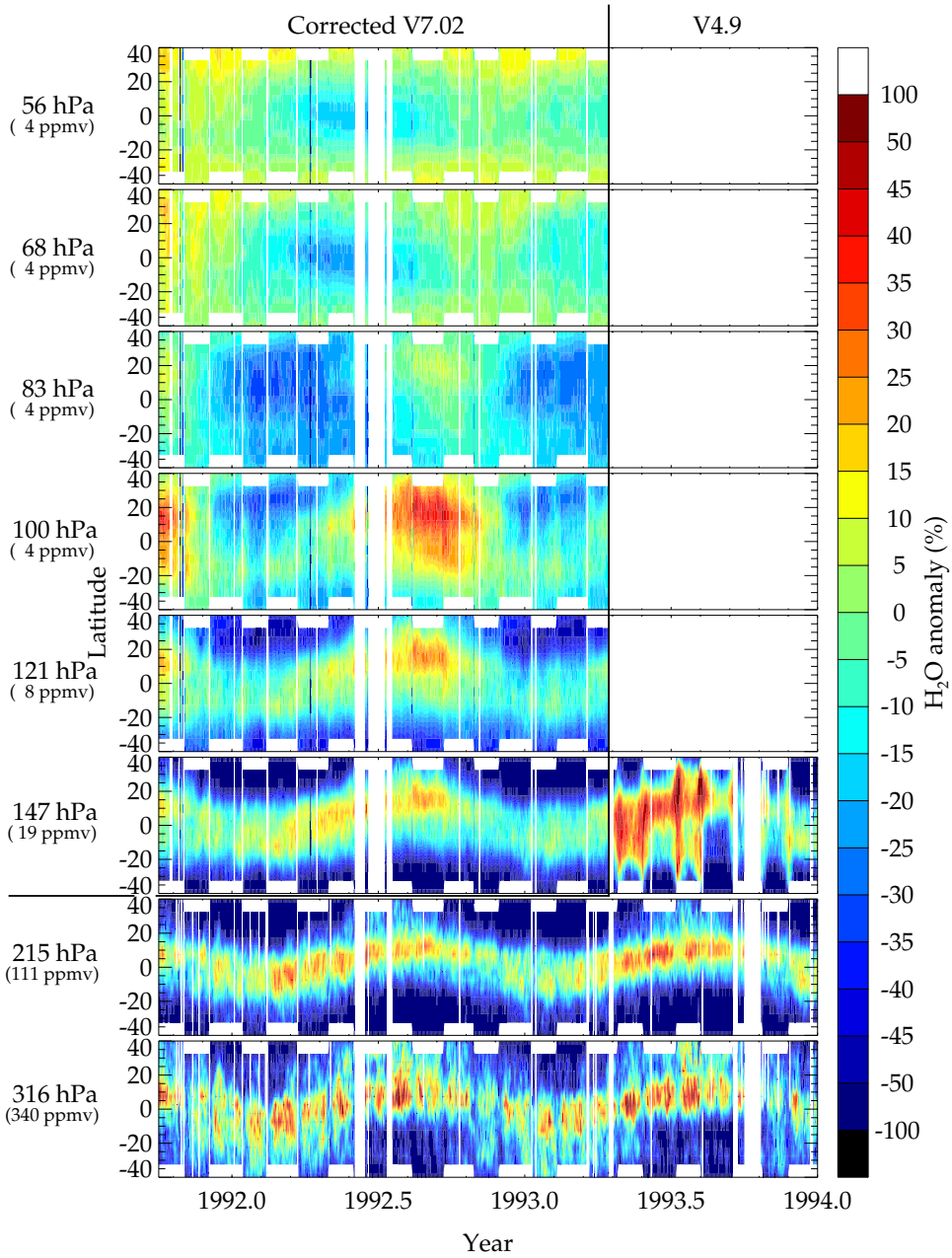

Figure 1. Time series of the H_2O zonal mean for several heights measured by MLS. V7.02 data were used for 147–56 hPa, and V4.9 data were used for 316, 215, and 147 hPa after April 1993. The V7.02 147 hPa and 100 hPa levels are increased by 30 and 20%, respectively, to remove likely biases at these pressures [*Read et al.*, 2004]. The colors represent a percent change relative to the value in parentheses. The parenthetical value is the 12°S to 12°N H_2O layer mean rounded to the nearest ppmv for pressures greater than 100 hPa or is the tropical stratospheric entry H_2O rounded to the nearest ppmv [*Dessler and Kim*, 1999] for pressures less than or equal to 100 hPa.

perature from March to August between 147 hPa and 100 hPa. A value of 2 K was subtracted from all the UKMO 100 hPa temperature to account for a warm bias at the tropical tropopause [*Randel et al.*, 2000]. The daily average UKMO temperatures between 12°S and 12°N at 147, 100, 68 hPa from January 1991 to May 1993 are computed. The average temperatures were smoothed using the [*Zeng and Levy*, 1995] algorithm over a 10-day temporal range. The 147, 100, and 68 hPa UKMO temperatures serve as the model input temperatures at 14, 16.5, and 19 km, respectively. We ignore the likelihood that the three UKMO pressures and temperatures are not in hydrostatic balance with their assigned heights. The temperature field for intermediate levels in the model was obtained from linear interpolation of the model input temperatures at 14, 16.5 and 19 km. As in the study by *Holton and Gettelman* [2001], a cold pool is modeled by superimposing a 2-D Gaussian perturbation function centered at 16.5 km (tropopause) with a 2500 km horizontal and 1 km vertical widths on the background temperature

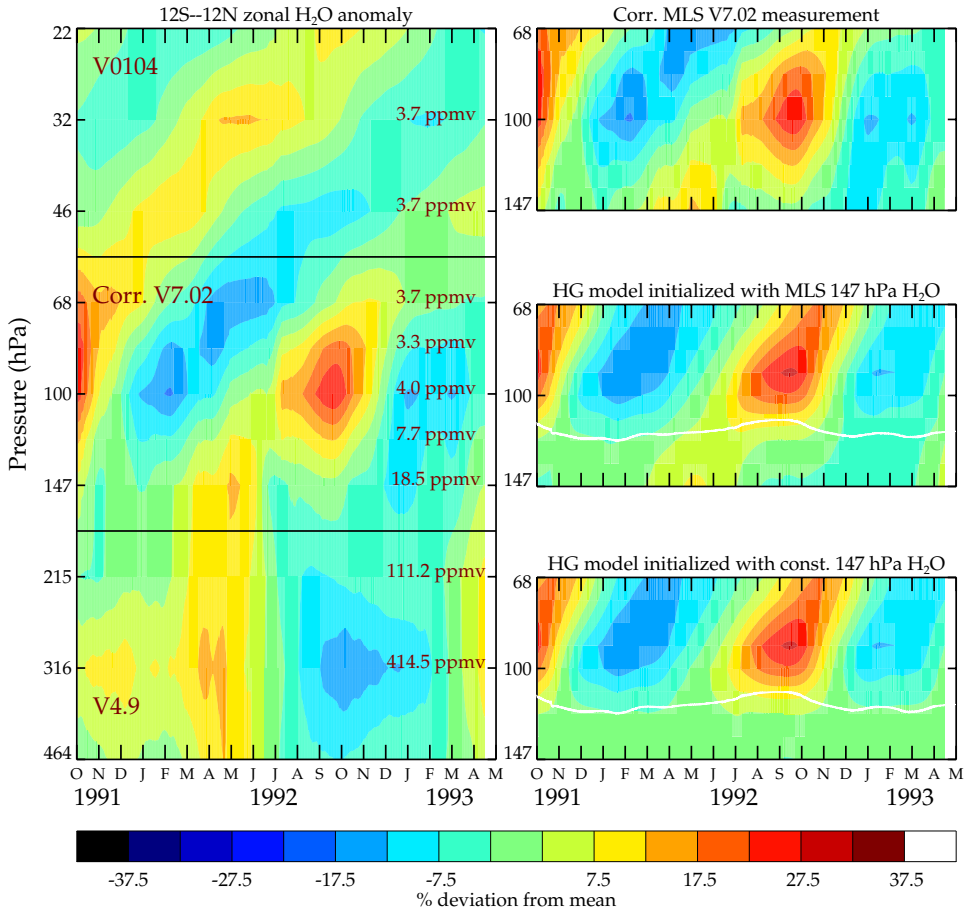

Figure 2. A time-height H_2O anomaly contour plot for the tropics. The left panel is a composite from the V4.9, V7.02, and V0104 data sets. MLS V4.9 data are used for pressure levels of 215 hPa and greater, and V0104 data are used for pressures of 46 hPa and less. Colors show the percentage deviation at each level from its mean value (given on the right side of the plot). The 147 and 100 hPa data used to construct this figure were increased by 30 and 20%, respectively, to account for a likely dry bias [*Read et al.*, 2004]. The data have been temporally smoothed, as discussed in the text, to remove short-term fluctuations. The upper right panel is the MLS measurement between 147 and 68 hPa, repeated to facilitate comparison with model results, the center right panel is a result from the *Holton and Gettelman* [2001] model that uses the time-varying 147 hPa MLS V7.02 H_2O measurements entering the TTL from below, and the bottom right panel is a result from the *Holton and Gettelman* [2001] model using 18.5 ppmv H_2O (the annual mean of the 147 hPa MLS V7.02 H_2O measurement) entering the TTL. The vertical profiles from the model were smoothed to match the vertical resolution of the MLS. The thick white lines show the altitude of the peak in the modeled ice layer.

profile. The amplitude of the perturbation is the difference between the daily minimum and average 100 hPa UKMO temperature between 12°S and 12°N at 100 hPa. The 100 hPa UKMO daily minimum temperature is smoothed similarly to the UKMO daily temperature average. The vertical velocity over the cold pool region is also perturbed by superimposing a 2-D Gaussian (same spatial parameters) on the background values. The perturbation amplitude of -0.4 mm s^{-1} allows a maximum velocity of -0.1 mm s^{-1} to account for radiative cooling from subvisible cirrus lying above the deep convective anvils in the cold trap [*Hartmann et al.*, 2001]. As H_2O advects upward into a lower temperature and exceeds 100% relative humidity with respect to ice, ice is formed with a condensation time constant of 1 $hour^{-1}$. Ice falls at -4 mm s^{-1} and evaporates with a time constant of 1 day^{-1}. The model also includes vertical diffusion and extratropical mixing. Water vapor at the bottom boundary of the model (14 km) is either the daily 12°S to 12°N 147 hPa MLS V7.02 average increased by 30% and smoothed over 10 days or is the October 1991 to April 1993 12°S to 12°N average MLS 147 hPa H_2O increased by 30%. The model has 37 horizontal grid points (500 km spacing) and 61 vertical levels (0.083 km spacing). The time step for the advection and the H_2O vapor/ice partitioning scheme is 2 hours. The pressures for every horizontal grid point for each day are computed from hydrostatic balance using 150 hPa as the reference pressure at 14 km. The daily zonal mean is computed by vertically interpolating the H_2O profile for each horizontal grid point onto a regular base 10 logarithm of pressure grid having 9 equally spaced values between 2.17 (147 hPa) and 1.83 (68 hPa) and

averaging over the horizontal coordinate. Except for the bottom boundary H_2O and the longitude-height-time temperature fields, the parameterizations are identical to *Holton and Gettelman* [2001].

[9] The model run was started with 1 January 1991 and run through 15 April 1993. The three right-hand panels in Figure 2 show the (top) V7.02 measurement and (center and bottom) results from two model calculations, all panels having the same vertical and temporal extent. The center-right panel shows a model run where moisture entering the TTL from below is constrained to the daily 12°S to 12°N 10-day smoothed average of the MLS V7.02 147 hPa H_2O. For the period from the 1 January 1991 to 2 October 1991 period (when V7.02 data are not available) we used MLS data from the following year for the TTL entry-level values. The bottom panel shows a model run that used a constant 18.5 ppmv (the average of all MLS V7.02 147 hPa H_2O measured between 12°S and 12°N increased by 30%) as the entry H_2O value into the TTL. The model results have been vertically smoothed by 0.187 log(hPa) (3 km) to emulate the vertical smoothing inherent in the MLS measurements.

[10] Agreement, throughout the TTL, is good between MLS observations and the *Holton and Gettelman* [2001] model using 147 hPa V7.02 H_2O as the lower boundary condition. Noteworthy are the ''bridges'' of near zero or slightly positive anomalies that lie between 147 and 215 hPa and bisect the upward propagating dry phase between October to April. The model also produces similar features between 147 and 121 hPa, just below the peak of the ice concentrations. The source of these bridges in the model is evaporation of falling ice. The modeled ''bridge'' is more moist in 1992 than in 1993, in agreement with the MLS observations. Another feature is the local minimum in the relative amplitude observed in the upward propagating moist phase between 147 and 100 hPa. This feature is captured by the model (near ~121 hPa). Evaporation of falling ice during the cold dry phase acts to reduce the relative seasonal cycle amplitude of H_2O at 121 hPa. There was more moisture entering the TTL in late 1991/early 1992 than in the following year, which might be expected to lead to more ice formation and subsequently more evaporative moistening during the first year of observation than in the second, as seen both by MLS and the model. Our run of the model results in a layer of ice ~1 km thick centered at ~15.5 km that is present in the cold pool throughout the year. The modeled ice concentration during the Northern Hemisphere (NH) winter is greater than during the NH summer, consistent with Stratospheric Aerosol and Gas Experiment (SAGE) II observations of subvisible cirrus [*Wang et al.*, 1996].

[11] The much poorer agreement below 100 hPa obtained from the model run using a constant value for the lower boundary is evidence that temperature variations (as portrayed in the UKMO data, which capture the phase change in the temperature maximum from March to August), and changes in H_2O phase that result from them, cannot be the cause of the upward propagating positive H_2O anomaly feature connecting the base of the TTL and the tropopause. Temperature variations can only impart a 6% peak to peak anomaly in H_2O. This feature is consistent with gradual ascent of H_2O from below, as the model run initialized with temporally varying 147 hPa H_2O shows. Both model runs show virtually identical results at and above 100 hPa, in good agreement with observations and consistent with H_2O near and above the tropopause being regulated by the minimum tropopause temperature. This suggests that the stratospheric water vapor content in the tropics is not sensitive to the amount of water vapor entering the TTL. The observations also show a deeper dry phase above 100 hPa in January 1992 than in January 1993, a feature well reproduced in both model runs. The cause of this difference is, apparently, a colder tropopause in January 1992 than in January 1993.

[12] The good agreement between the MLS observations and the *Holton and Gettelman* [2001] model is consistent with in situ dehydration in the TTL by rapid horizontal processing through a cold pool, coupled with gradual ascent. This does not eliminate convection as being important. Our results show that in the subtropopause TTL, far better agreement is achieved with MLS observations when the model lower boundary uses the measured temporally varying upper tropospheric H_2O. This apparently requires that the height of convection must reach at least to the base of the TTL since *Sherwood and Dessler* [2003] show that having convection capped below the TTL would eliminate the seasonal variation in H_2O entering the TTL. They found the best fit to measurements of the amplitude and seasonal cycle for CO_2 occur when convection reaches 0.5–1 km below the tropopause.

[13] Of particular interest is whether overshooting convection can also be a primary TTL dehydration mechanism [*Sherwood and Dessler*, 2001]. A representative run of a convective overshooting model [*Sherwood and Dessler*, 2003] shows a maximum in the relative amplitude of the H_2O seasonal cycle occurring slightly above the base (140–130 hPa) of the TTL that monotonically decays with increasing altitude. Ice condensed in the overshoot enters the TTL near its base where the detrainment timescale is shorter than the clear-sky advection timescale. The detrained ice evaporates at a rate approximately inversely proportional to the background relative humidity in the convective overshooting model. The seasonal variability in background relative humidity (follows temperature) modulates the amount of evaporation and leads to a maximum in the relative amplitude of H_2O near the base of the TTL. As the water vapor slowly advects upward its concentrations are steadily reduced as it mixes with very dry overshooting air. Dilution with dry overshooting air and vertical diffusion lead to a monotonic decay of the relative seasonal cycle amplitude with altitude. It appears that this simple convective model cannot explain either the maximum in the relative seasonal cycle amplitude in H_2O occurring near 100 hPa or the minimum in percent deviation from the mean at ~121 hPa observed by MLS in the upward-propagating moist phase. More model work, and MLS observations over a longer period (that will be available starting in 2004 from the NASA Aura mission), are needed to investigate this issue. In-situ dehydration currently provides the simplest explanation of the MLS observations of the temporally varying vertical distribution of H_2O in the TTL.

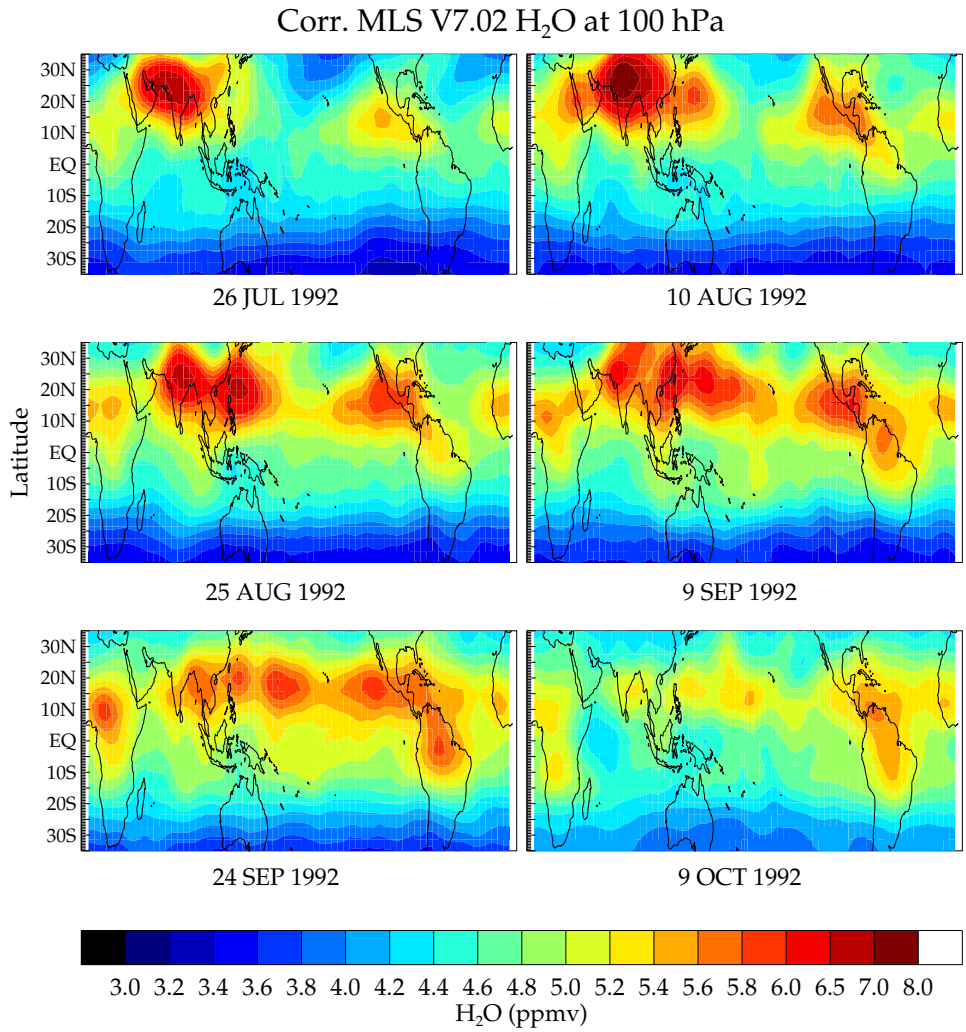

Figure 3. Evolution of the corrected MLS V7.02 100 hPa H_2O from 17 July 1992 to 16 October 1992. Each map is a 15-day average of MLS observations centered at the indicated dates.

[14] Figure 3 present a series of 15-day H_2O maps from 17 July to 16 October 1992 at 100 hPa showing the moisture evolution during the Indian and North American monsoon periods. Enhanced H_2O occurs over India in July and August 1992. This moisture enhancement appears to move toward southeast Asia and weaken over a period of roughly 6 weeks. Enhanced moisture associated with the North American monsoon is weaker and is strongest from late August to mid-September 1992. The monsoon-related features occur near 20°N, appear isolated from the tropics, and do not seem to migrate equatorward. Therefore the high-zonal-mean anomaly at 100 hPa in Figure 2 does not appear to be appreciably influenced by influx associated with the Northern Hemisphere monsoons. By end of September, and into October 1992, tropical H_2O is decreasing.

[15] Figures 4 and 5 show seasonal maps of MLS V7.02 H_2O at 100 hPa and 83 hPa, levels that straddle the NH winter tropical tropopause [*Reid and Gage*, 1996]. Regions of lowest 100 hPa temperatures (UKMO) and outgoing longwave radiation (OLR, from the NOAA-CIRES Climate Diagnostics Center web site, http://www.cdc.noaa.gov/) less than 220 W m^{-2} are overlaid. The OLR contours enclose regions where deep convection is active. Tropical 100 hPa H_2O concentrations follow the seasonal temperature variation. The 83 hPa H_2O concentrations lag the temperature and 100 hPa H_2O concentrations by a season.

[16] December-January-February (DJF) 100 hPa maps for both years of MLS data show a deep minimum in H_2O at 20°N and a shallower minimum at 35°S. DJF 1991/92 was drier than DJF 1992/3. The HALOE multiyear climatology shows a zonal deep minimum that is slightly south of 20°N [*Gettelman et al.*, 2002]. The DJF MLS 100 hPa maps show more zonal symmetry than HALOE V19 and in particular, there is a band of relatively moist values at 15°S. OLR contours indicate that this is an active convective region and H_2O at 147 and 121 hPa are high. Vertical resolution of MLS may be smearing some of the lower altitude water vapor into the 100 hPa level. A latitude versus height climatology composite of HALOE V19 H_2O, frequencies of deep convection, mean meridional circulations, and temperature in the western Pacific for DJF shows convection and the cold pool south of the lowest H_2O with the mean Hadley circulation bringing air up where frequency of convection is highest through the cold pool and then heading north across the equator where H_2O is lowest [*Randel et al.*, 2001]. The MLS maps appear consistent

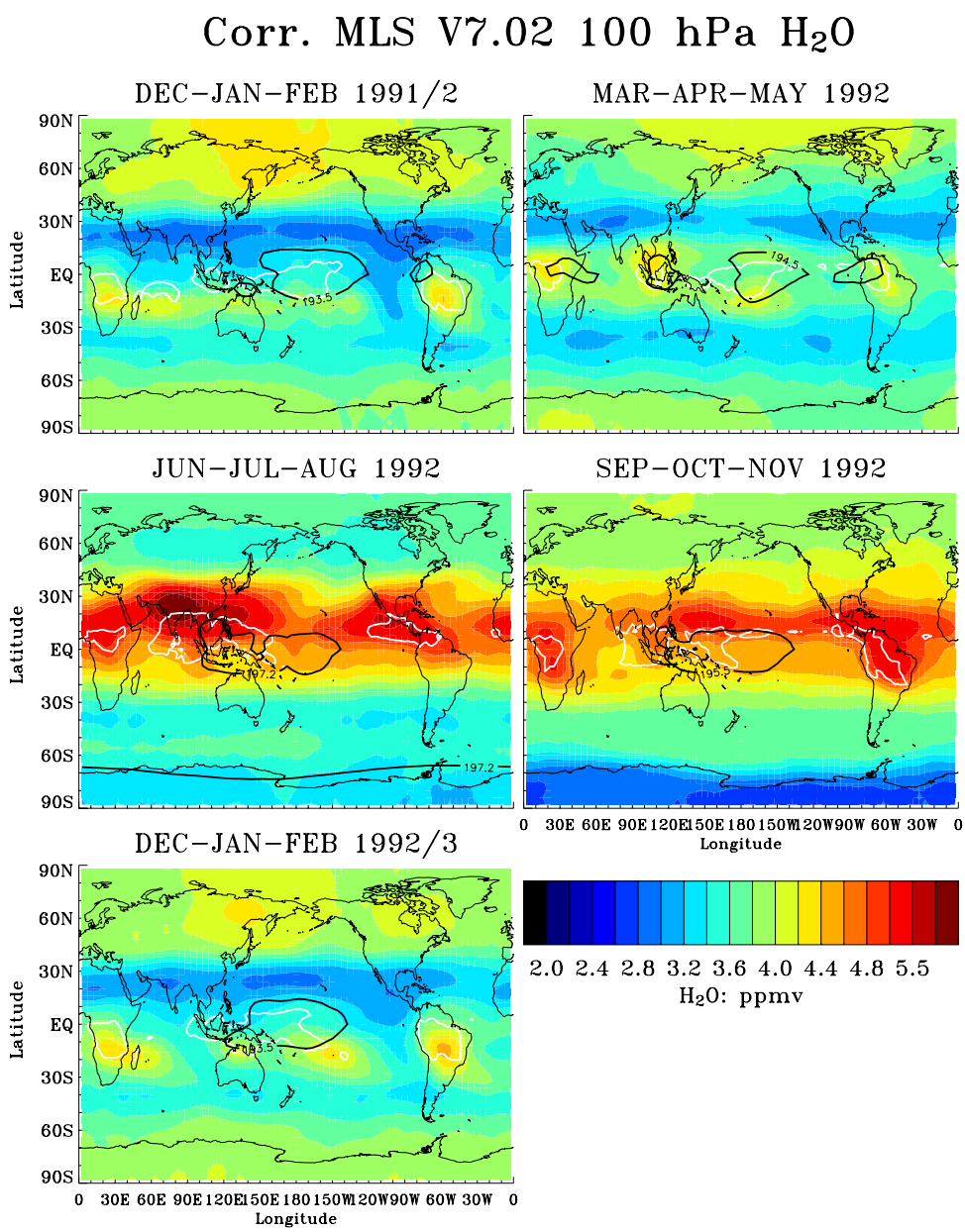

Figure 4. MLS seasonal maps of H_2O at 100 hPa increased by 20% to reduce a likely dry bias [*Read et al.*, 2004]. UKMO 100 hPa temperatures (2 K bias not removed) of 193.5 K for DJF, 194.5 for MAM, 197.2 K for JJA, and 195.5 for SON are indicated by the black contours. Regions where outgoing longwave radiation is less than 220 W m^{-2} are indicated by the white contours.

with the circulation pattern shown by *Randel et al.* [2001]: low H_2O at 83 hPa nearly coincident with lowest tropopause temperature and somewhat northward of deep convection with the 100 hPa dry pool northward (and possibly southward) of deep convection. As shown by *Randel et al.* [2001], the driest region at 100 hPa may be downstream of the lowest tropopause temperature and maritime deep convection region. A zonal vertical cross section of MLS H_2O over the western Pacific averaged over January 1992 and 1993 is shown in Figure 6 is consistent with *Randel et al.* [2001]. The *Gettelman et al.* [2002] 3-D trajectory model (which contains a simple microphysical model, a stochastic temperature perturbation to simulate gravity waves, and is driven by ECMWF wind and temperature analyses) produces a 100 hPa H_2O map that agrees well with the MLS 83 hPa map but not with the MLS 100 hPa map. The model tends to place the zonal band of lowest 100 hPa H_2O closer to the equator than either HALOE or MLS. Causes of these differences might be related to the tropopause height for which the model assumes 100 hPa, but in reality is higher [*Reid and Gage*, 1996], and the vertical smoothing in the MLS data. The MLS data indicate higher 100 and 83 hPa H_2O regions coinciding with deep convection over Africa and South America.

[17] March-April-May (MAM) 1992 shows a moistening of the tropics at 100 hPa, relative to DJF, consistent with warming of the cold pool temperature. H_2O at 83 hPa is drier than for DJF, caused by the tape recorder ascent of

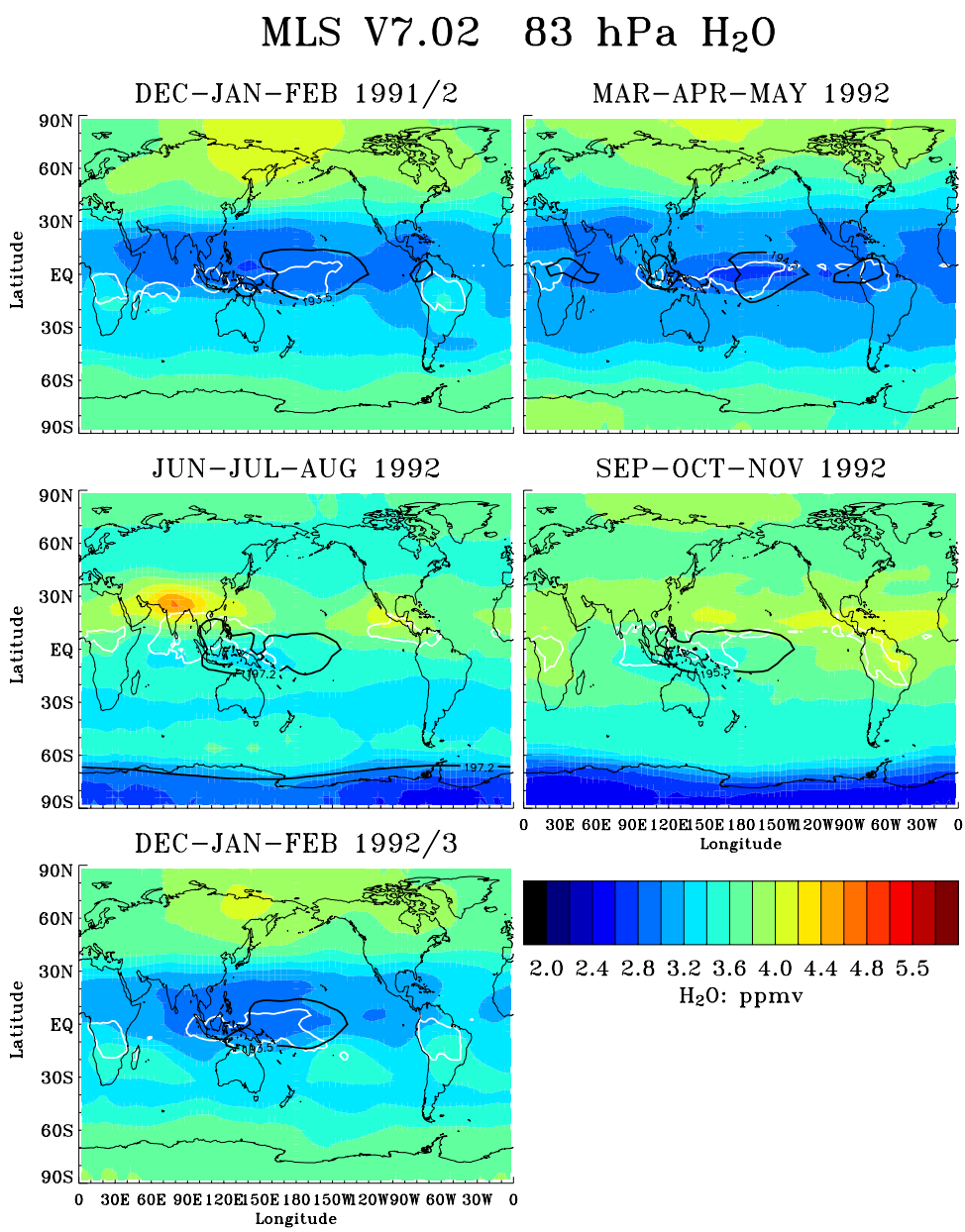

Figure 5. Same as Figure 4 except H_2O is at 83 hPa.

desiccated air. The tropical and extratropical 100 hPa H_2O in MAM has a similar distribution to that in DJF but is more symmetric about the equator.

[18] June-July-August (JJA) 1992 has, of all the MLS seasonal maps, the largest values of tropical 100 and 83 hPa H_2O, centered at approximately 20°N, which is northward of the regions of deep convection and lowest temperatures. The tropical morphologies of H_2O at 100 and 83 hPa are very similar, which is not the case for DJF. The two maxima at ~20°N are associated with the Indian and North American monsoons. These features are also prevalent in the HALOE 100 hPa V19 multiyear climatology [*Gettelman et al.*, 2002]. Also consistent with HALOE is the latitude-dependent slope of decreasing H_2O, which is steeper at 100 hPa. HALOE shows a small region of low H_2O at 100 hPa east of Indonesia and coincident with the lowest 100 hPa temperatures. Apart from an equatorward deflection of the 4.4 ppmv contour in the maritime continent, this feature is not readily seen in the MLS V7.02 100 hPa H_2O map. This dry feature is simulated by the *Gettelman et al.* [2002] 3-D trajectory model. The lowest mapped tropical H_2O value for the corrected MLS is 4.4 ppmv, for HALOE (increased 10% to correct for its bias, an average of the biases between in situ and HALOE H_2O measurements at 100 hPa reported in section 2.3.1 of *Kley et al.* [2000]) is 4.2 ppmv, and for the *Gettelman et al.* [2002] model is 3.8 ppmv.

[19] September-October-November (SON) has tropical 100 hPa H_2O abundances less than the JJA values. Tropical 83 hPa H_2O has increased relative to JJA, reflecting the slow-ascent of H_2O that passed through a warmer tropopause. Both heights have a tropical zonal structure that is similar to JJA. The cold pool is ~1 K warmer than in MAM. The 100 hPa H_2O does not show a

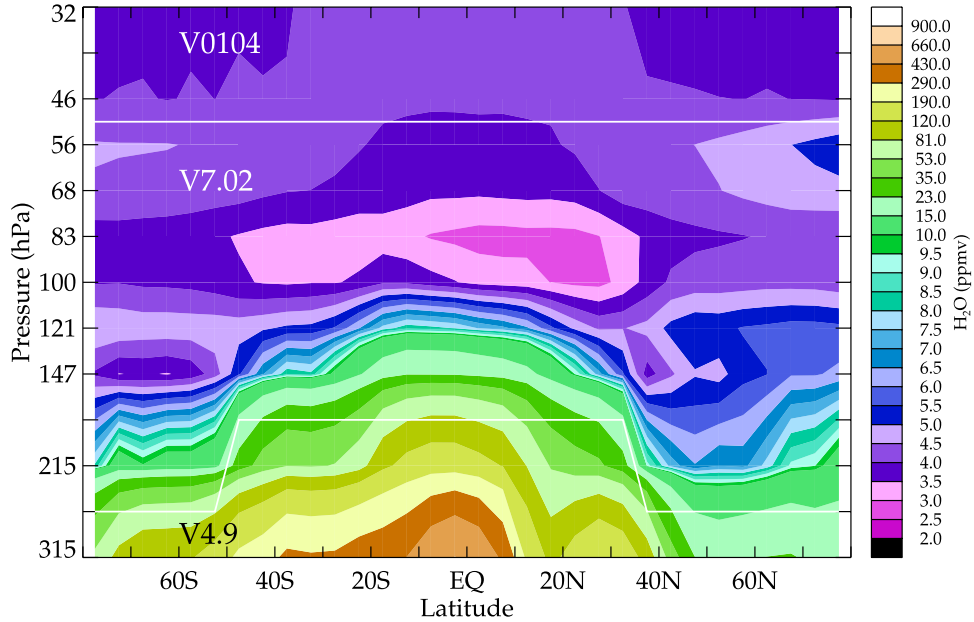

Figure 6. Zonal cross section of H_2O over the western Pacific (120°E to 180°) averaged over January 1992 and 1993. The 147 and 100 hPa H_2O are increased by 30 and 20%, respectively, to remove measurement biases [*Read et al.*, 2004]. White lines indicate the altitude ranges of the respective data set used to produce the figure.

clear connection with either deep convection or low temperature, but 83 hPa H_2O does show a connection. An important difference between the 100 and 83 hPa H_2O maps is that the 100 hPa appears to have ongoing dehydration and the air is under the influence of tropospheric circulations (e.g., Hadley rising, sinking, and meridional transport [*Randel et al.*, 2001]) whereas the 83 hPa, dehydration is (mostly) complete and air is slowly rising, following the stratospheric Brewer-Dobson circulation. The differences between the 100 and 83 hPa show most distinctly in DJF when the tropopause is above 100 hPa in the tropics [*Randel et al.*, 2000].

[20] Throughout the year, the highest tropical 100 hPa H_2O occurs over the continents and is usually aligned with deep convection. Tropical %RHi at 100 hPa (D. Wu et al., UARS MLS cloud ice measurements and implications for H_2O transport near the tropopause, submitted to *Journal of Atmospheric Science*, 2003) is also highest over the continents. It seems unlikely, therefore, that deep convection over continents is drying the TTL. The higher %RHi values over the continents may be a result of smaller ice sizes [*Sherwood*, 2002], which would cause convection to dehydrate relatively less efficiently over land than ocean.

4. Conclusions

[21] The zonal mean H_2O from 316 to 100 hPa has a maximum following the solar seasonal cycle with a two month lag, indicating influence from tropical deep convection. The data are consistent with slow ascent beginning near 147 hPa, the bottom of the TTL, and a decrease in the relative amplitude in the seasonal cycle from 147 hPa to 121 hPa. A maximum in the relative amplitude in the seasonal cycle of H_2O is seen to occur at 100 hPa. All the major features observed in the time-height H_2O zonal means in the TTL are well reproduced by the *Holton and Gettelman* [2001] "cold-trap" model using the MLS 147 hPa H_2O measurements as the lower boundary condition and UKMO temperatures reduced by 2 K. The requirement of needing the time resolved MLS 147 hPa H_2O measurements at the base of the TTL to obtain good agreement with the measurement below the tropopause is evidence that convection is necessary for supplying H_2O into the TTL (assuming negligible horizontal transport from the extratropics) [*Sherwood and Dessler*, 2003].

[22] The MLS 147-100 hPa H_2O observations appear not to be consistent with results from a representative time-evolved model employing overshooting convection as the primary dehydration mechanism, which predicts the maximum relative amplitude in the seasonal cycle of H_2O occurring near the base of the TTL with gradual decay at higher altitudes [*Sherwood and Dessler*, 2003]. The near-constant value for the HDO/H_2O ratio measured by the Atmospheric Trace Molecule Spectroscopy (ATMOS) spectrometer [*Gunson et al.*, 1996] over 12–22 km in the tropics, on the other hand, appears inconsistent with TTL dehydration by gradual in situ processes [*Kuang et al.*, 2003], implying a major role by convection, and shown to be consistent with the overshooting dehydration mechanism [*Dessler and Sherwood*, 2003]. Recent in situ observations by *Webster and Heymsfield* [2003], however, show a wide range of isotopic fractions providing evidence for convective ice lofting and in situ formation. The *Webster and Heymsfield* [2003] observations show that if 22% of the stratospheric H_2O originates from evaporated lofted ice, then in situ freeze-drying is consistent with the observed HDO/H_2O ratios seen in the stratosphere. They also show that when the aircraft data are cloud-screened

and averaged over the ATMOS resolution the data are consistent with a constant HDO/H_2O ratio in the TTL.

[23] The seasonal evolution of the MLS V7.02 100 hPa H_2O from the end of 1991 to early 1993 show general features similar to those seen by HALOE [*Gettelman et al.*, 2002], but with a notable difference. The DJF (and MAM) maps at 100 hPa show a second (albeit less dry) water vapor minimum at 35°S and a zonal band of higher H_2O aligned with tropical convection. These MLS data appear consistent with tropospheric circulations and a tropopause <100 hPa as given by *Randel et al.* [2000, 2001]. Both zonal dry features are absent at 83 hPa. It could be that in DJF the 100 hPa H_2O is completing dehydration and is under the influence of more complex dynamics where air is rising and sinking following the tropospheric Hadley circulation patterns, with some of the 100 hPa air destined for the stratosphere. Air at 83 hPa, could be dominated by the Brewer-Dobson circulation with all the air destined for the stratosphere.

[24] The low-water-vapor features at 83 hPa are closely aligned with the region of minimum tropopause temperatures and maritime deep convection. Higher tropical 100 hPa (and sometimes 83 hPa) H_2O is associated with deep convection over land. Therefore it seems unlikely that deep convection over land could be drying the TTL. It appears that only overshooting in maritime continent deep convection and/or the tropopause cold pool, which are closely associated with low water vapor at 83 hPa, could be desiccating the air entering the stratosphere. The 100 hPa H_2O difference associated with land versus oceanic convection appears consistent with the microphysical connections discussed by *Sherwood* [2002].

[25] An improved MLS will be on the Earth Observing System's (EOS) Aura satellite to be launched in 2004 with an operational lifetime of 5 years or more. Unlike UARS MLS, which was not designed for measurement of tropospheric and lower stratospheric H_2O, EOS MLS is designed to measure H_2O throughout the upper troposphere, stratosphere and mesosphere. The expected EOS MLS measurement precision for individual H_2O profiles retrieved at 6 levels per decade change in pressure (2.7 km) is 0.1–0.15 ppmv with a vertical resolution of 2.8 km in the TTL region. For H_2O profiles retrieved at 12 levels per decade (1.4 km), the precision is 2–3 ppmv with a vertical resolution of 2.1 km in the TTL.

[26] **Acknowledgments.** We thank A. E. Dessler, A. Gettleman, J. R. Holton, P. W. Mote, R. Salawitch, and S. C. Sherwood for helpful discussions, J. R. Holton for providing details of the *Holton and Gettelman* [2001] 2-D TTL model, Gloria Manney for her regridded files of UKMO temperatures, N. Livesey and M. Filipiak for the precision versus resolution data for the EOS MLS, and two anonymous referees for their comments and suggestions. This work was part of an effort at developing algorithms for retrieving H_2O in the TTL from measurements by EOS MLS to be launched in 2004 on the Aura satellite, and we thank M. R. Schoeberl, Aura Project Scientist, for encouraging and supporting our efforts in this area. The research described here done at the Jet Propulsion Laboratory, California Institute of Technology, was under contract with the National Aeronautics and Space Administration.

References

Barath, F. T., et al. (1993), The Upper Atmosphere Research Satellite Microwave Limb Sounder Instrument, *J. Geophys. Res.*, *98*, 10,751–10,762.

Dessler, A. E., and H. Kim (1999), Determination of the amount of water vapor entering the stratosphere based on Halogen Occultation Experiment (HALOE) data, *J. Geophys. Res.*, *104*, 30,605–30,607.

Dessler, A. E., and S. C. Sherwood (2003), A model of HDO in the tropical tropopause layer, *Atmos. Chem. Phys.*, *3*, 2173–2181.

Elson, L. S., W. G. Read, J. W. Waters, P. W. Mote, J. S. Kinnersley, and R. S. Harwood (1996), Space-time variations in water vapor as observed by the UARS Microwave Limb Sounder, *J. Geophys. Res.*, *101*, 9001–9015.

Gettelman, A., W. J. Randel, F. Wu, and S. T. Massie (2002), Transport of water vapor in the tropical tropopause, *Geophys. Res. Lett.*, *29*(1), 1009, doi:10.1029/2001GL013818.

Gunson, M. R., et al. (1996), The Atmospheric Trace Molecule Spectroscopy (ATMOS) experiment: Deployment on the ATLAS Space Shuttle missions, *Geophys. Res. Lett.*, *23*, 2333–2336.

Hartmann, D. L., J. R. Holton, and Q. Fu (2001), The heat balance of the tropical tropopause, cirrus, and stratospheric dehydration, *Geophys. Res. Lett.*, *28*, 1969–1972.

Holton, J. R., and A. Gettelman (2001), Horizontal transport and the dehydration of the stratosphere, *Geophys. Res. Lett.*, *28*, 2799–2802.

Holton, J. R., P. H. Haynes, M. E. McIntyre, A. R. Douglass, R. B. Rood, and L. Pfister (1995), Stratosphere-troposphere exchange, *Rev. Geophys.*, *33*, 403–439.

Jensen, E. J., W. G. Read, J. Mergenthaler, B. J. Sandor, L. Pfister, and A. Tabazadeh (1999), High humidities and subvisible cirrus near the tropical tropopause, *Geophys. Res. Lett.*, *26*, 2347–2350.

Kley, D., J. M. Russell III, and C. Phillips (2000), SPARC assessment of upper tropospheric and stratospheric water vapour, *SPARC Rep. 2, WCRP-113*, WMO/ICSU/IOC, Cent. Natl. de la Rech. Sci., Verrières le Buisson, France.

Kuang, Z., G. C. Toon, P. O. Wennberg, and Y. L. Yung (2003), Measured HDO/H_2O ratios across the tropical tropopause, *Geophys. Res. Lett.*, *30*(7), 1372, doi:10.1029/2003GL017023.

Mote, P. W., K. H. Rosenlof, J. R. Holton, R. S. Harwood, and J. W. Waters (1995), Seasonal variations of water vapor in the tropical lower stratosphere, *Geophys. Res. Lett.*, *22*, 1093–1096.

Mote, P. W., et al. (1996), An atmospheric tape recorder: The imprint of tropical tropopause temperatures on stratospheric water vapor, *J. Geophys. Res.*, *101*, 3989–4006.

Nedoluha, G. E., R. M. Bevilacqua, R. M. Gomez, B. C. Hicks, J. M. Russell III, and B. J. Connor (2003), An evaluation of trends in middle atmospheric water vapor as measured by HALOE, WVMS, and POAM, *J. Geophys. Res.*, *108*(D13), 4391, doi:10.1029/2002JD003332.

Pumphrey, H. C. (1999), Validation of a new prototype water vapor retrieval for the UARS Microwave Limb Sounder, *J. Geophys. Res.*, *104*, 9399–9412.

Randel, W. J., F. Wu, and D. J. Gaffen (2000), Interannual variability of the tropical tropopause derived from radiosonde data and NCEP reanalyses, *J. Geophys. Res.*, *105*, 15,509–15,523.

Randel, W. J., F. Wu, A. Gettelman, J. M. Russell III, J. M. Zawodny, and S. J. Oltmans (2001), Seasonal variation of water vapor in the lower stratosphere observed in Halogen Occultation Experiment data, *J. Geophys. Res.*, *106*, 14,313–14,325.

Read, W. G., et al. (2001), UARS MLS upper tropospheric humidity measurement: Method and validation, *J. Geophys. Res.*, *106*, 32,207–32,258.

Read, W. G., D. L. Wu, J. W. Waters, and H. C. Pumphrey (2004), A new 147–56 hPa water vapor product from the UARS Microwave Limb Sounder, *J. Geophys. Res.*, *109*, D06111, doi:10.1029/2003JD004366.

Reber, C. A. (1993), The Upper Atmosphere Research Satellite, *Geophys. Res. Lett.*, *20*, 1215–1218.

Reed, R., and C. L. Vleck (1969), The annual temperature variation in the lower tropical stratosphere, *J. Atmos. Sci.*, *26*, 163–167.

Reid, G. C., and K. S. Gage (1996), The tropical tropopause over the western Pacific: Wave driving, convection, and the annual cycle, *J. Geophys. Res.*, *101*, 21,233–21,241.

Rosenlof, K. H. (2002), Transport changes inferred from HALOE water and methane measurements, *J. Meteorol. Soc. Jpn.*, *80*, 831–848.

Rosenlof, K. H., et al. (2001), Stratospheric water vapor increases over the past half-century, *Geophys. Res. Lett.*, *28*, 1195–1198.

Russell, J. M., III, et al. (1993), The Halogen Occultation Experiment, *J. Geophys. Res.*, *98*, 10,777–10,798.

Seidel, D. J., R. J. Ross, J. K. Angell, and G. C. Reid (2001), Climatological characteristics of the tropical tropopause as revealed by radiosondes, *J. Geophys. Res.*, *106*, 7857–7878.

Sherwood, S. C. (2002), A microphysical connection among biomass burning, cumulus clouds, and stratospheric moisture, *Science*, *295*, 1272–1275.

Sherwood, S. C., and A. E. Dessler (2000), On the control of stratospheric humidity, *Geophys. Res. Lett.*, *27*, 2513–2516.

Sherwood, S. C., and A. E. Dessler (2001), A model for transport across the tropical tropopause, *J. Atmos. Sci.*, *58*, 765–779.

Sherwood, S. C., and A. E. Dessler (2003), Convective mixing near the tropical tropopause: Insights from seasonal variations, *J. Atmos. Sci.*, *60*, 2674–2685.

Wang, P.-H., P. Minnis, M. P. McCormick, G. S. Kent, and K. M. Skeens (1996), A 6-year climatology of cloud occurrence frequency from Stratospheric Aerosol and Gas Experiment II observations (1985–1990), *J. Geophys. Res.*, *101*, 29,407–29,429.

Waters, J. W., et al. (1999), The UARS and EOS Microwave Limb Sounder experiments, *J. Atmos. Sci.*, *56*, 194–218.

Webster, C. R., and A. J. Heymsfield (2003), Water isotope ratios D/H, $^{18}O/^{16}O$, $^{17}O/^{16}O$ in and out of clouds map dehydration pathways, *Science*, *302*, 1742–1745.

Yulaeva, E., J. R. Holton, and J. M. Wallace (1994), On the cause of the annual cycle in tropical lower-stratospheric temperatures, *J. Atmos. Sci.*, *51*, 169–174.

Zeng, L., and G. Levy (1995), Space and time aliasing structure in monthly mean polar-orbiting satellite data, *J. Geophys. Res.*, *100*, 5133–5142.

H. C. Pumphrey, Department of Meteorology, University of Edinburgh, James Clerk Maxwell Building, King's Buildings, Mayfield Road, Edinburgh EH9 3JZ, UK. (h.c.pumphrey@ed.ac.uk)

W. G. Read, J. W. Waters, and D. L. Wu, Jet Propulsion Laboratory, Mail Stop 183-701, 4800 Oak Grove Drive, Pasadena, CA 91109, USA. (bill@mls.jpl.nasa.gov; joe@mls.jpl.nasa.gov; dwu@mls.jpl.nasa.gov)